Geophysical Research Letters

RESEARCH LETTER
10.1029/2021GL096708

Improved Representation of Extratropical Cyclone Structure in HighResMIP Models

Matthew D. K. Priestley[1] and **Jennifer L. Catto**[1]

[1]College of Engineering, Mathematics and Physical Sciences, University of Exeter, Exeter, UK

Key Points:

- The strength of cyclone wind speeds are underestimated by CMIP6 models
- HighResMIP models represent the structure and intensity of cyclones better than CMIP6 models
- Elements of the large-scale environment surrounding cyclones are not improved in HighResMIP simulations

Supporting Information:

Supporting Information may be found in the online version of this article.

Correspondence to:

M. D. K. Priestley,
m.priestley@exeter.ac.uk

Citation:

Priestley, M. D. K., & Catto, J. L. (2022). Improved representation of extratropical cyclone structure in HighResMIP models. *Geophysical Research Letters*, *49*, e2021GL096708. https://doi.org/10.1029/2021GL096708

Received 28 OCT 2021
Accepted 14 FEB 2022

Abstract General circulation models are broadly able to capture the shape and structure of extratropical cyclones. Increased atmospheric resolution has been shown to improve the representation of cyclone structure. However, the intensity of cyclones, and the strength of their winds, are commonly underestimated in models. Using a cyclone compositing technique applied to the new generation HighResMIP and CMIP6 models, the representation of cyclone wind speeds and airstreams is quantified. CMIP6 models are able to capture the structure of cyclones, however winds associated with various airstreams within the cyclones are too weak. HighResMIP models show considerable improvements, with a majority of cyclone-scale biases present in the CMIP6 models reduced in both winter and summer seasons in the Northern and Southern hemispheres. HighResMIP and CMIP6 models have similar biases on the large-scale, with both struggling to represent the width of the upper-level jet.

Plain Language Summary In order for accurate predictions of the future climate to be made, models must be tested to see if they reproduce features in an accurate way. In this study, we have tested the ability of climate models to represent the intensity and structure of extratropical cyclones. Previously, climate models with a higher resolution have performed better at representing the structure of these cyclones, however most models tend to fail to capture the intensity. Our results demonstrate that models do still struggle to capture the intensity of cyclones, with wind speeds being too weak. However, cyclones simulated by the highest resolution models do a much better job at simulating the intensity of the cyclones, and the strength of the wind speeds within them. In order to study features within extratropical cyclones accurately, high resolution models must be used.

1. Introduction

General Circulation Models (GCMs) are commonly capable of reproducing the structural features of extratropical cyclones (ETCs; Booth et al., 2018; Catto et al., 2010; Hawcroft et al., 2016). An accurate representation of ETCs is important in GCMs for current and future risk assessment as they are commonly associated with extreme wind (Browning, 2004), precipitation (Pfahl & Wernli, 2012), and waves (Catto & Dowdy, 2021). ETC structure is commonly viewed from an airstream (conveyor belt) perspective, with three main features. The first is the warm conveyor belt (WCB; Harrold, 1973), which is a stream of warm moist air ascending in the warm sector of ETCs. Second, the cold conveyor belt (CCB; Carlson, 1980; Schultz, 2001) is often confined to the lower troposphere and travels in the opposite direction to cyclone propagation. Finally, the dry intrusion (DI; Browning, 1997) is a dry air stream that descends from the upper troposphere or lower stratosphere (Raveh-Rubin, 2017), behind the cold front. For a more thorough review of cyclone airstreams and structure the readers are directed to Catto (2016) and Schultz et al. (2019).

ETCs are commonly evaluated using cyclone centered composites (Bengtsson et al., 2007, 2009; Booth et al., 2018; Catto et al., 2010; Dacre et al., 2012; Field & Wood, 2007; Kodama et al., 2019; Sinclair et al., 2020). Compositing methods have revealed that many features of ETCs are well represented in GCMs (Bengtsson et al., 2007; Booth et al., 2018; Catto et al., 2010; Govekar et al., 2014; Kodama et al., 2019). However, the wind speed strength is commonly underestimated (Govekar et al., 2014; Naud et al., 2010). Previous studies have often only considered individual models or a single hemisphere/region. There is a need to perform a systematic multi-model evaluation of cyclone wind speeds associated with the various airstreams in both hemispheres.

The new generation of models from the sixth phase of the Coupled Model Intercomparison Project (CMIP6; Eyring et al., 2016) tend to have higher resolutions than previously studied CMIP5 and CMIP3 models. Increasing atmospheric resolution has previously improved the simulation of cyclone intensity (Booth et al., 2018; Colle

et al., 2013; Jung et al., 2012; Willison et al., 2013), however, the highest resolution CMIP6 models still underestimate intensity relative to numerous reanalyzes (Priestley et al., 2020). CMIP6 models possess horizontal atmospheric resolution between 100 and 250 km (Taylor et al., 2017), yet current modeling capabilities allow for simulations with 25–50 km resolution, with these models participating in the HighResMIP project (Haarsma et al., 2016). HighResMIP models have shown improvements in the representation of blocking (Schiemann et al., 2020), simulated tropical cyclone intensity and frequency (Roberts et al., 2020), and in the number of explosive ETCs (Jiaxiang et al., 2020). It is hoped that any biases in ETC simulation in CMIP6, will be removed, or significantly reduced, in HighResMIP models.

In this study we address three questions:

1. Do CMIP6 models capture the structure and spatial extent of ETCs at the surface?
2. Are cyclone airstreams structurally captured by CMIP6 models and are they of sufficient strength?
3. What structural features are improved in HighResMIP models relative to CMIP6?

2. Data & Methods

Throughout this study, analysis will be performed on the December, January, February (DJF) and June, July, August (JJA) periods, representing the Northern Hemisphere (NH) winter and summer, and the Southern Hemisphere (SH) summer and winter respectively. All analysis will be conducted for the 1979–2014 period. The baseline data set used for the model evaluation is the ERA5 reanalysis (Hersbach et al., 2020).

2.1. CMIP6

The CMIP6 models used in this analysis are from the coupled *historical* simulations from the DECK set of experiments (Eyring et al., 2016). Models were used that provided zonal (u) and meridional (v) wind at 850-hPa and 250-hPa, as well as mean sea level pressure (MSLP, *psl*) at 6-hourly resolution. Whenever modeling centers have provided more than one model, a maximum of two models from that center are used in order to not over-weight a modeling group in the model mean. In cases when two models are used, they must have either different nominal resolutions for the atmospheric component or different atmospheric models (Taylor et al., 2017). This assumes that the model simulations are not overly similar. The CMIP6 models have nominal atmospheric resolution of either 100-km, 250-km, or 500-km resolution. In total 27 models are used from 20 model centers (see Table S1 in Supporting Information S1).

2.2. HighResMIP

The higher resolution set of model simulations are taken from the HighResMIP *hist-1950* experiment (Haarsma et al., 2016) and all are fully coupled with identical forcings to the *historical* experiments. A majority of the HighResMIP models have nominal atmospheric resolutions that are higher than the CMIP6 models, at 25-km, 50-km, or 100-km. In addition to the high resolution models, all modeling centers also provide a lower resolution model. These models are useful to directly identify the impact of resolution, have nominal resolutions comparable to the CMIP6 ensemble, and generally have grid spacing at least twice that of their high resolution counterpart. In total 6 high resolution models (and 6 low resolution counterparts) from 6 different modeling centers are used (Table S2 in Supporting Information S1).

2.3. Cyclone Identification, Tracking, and Compositing

Cyclones are identified and tracked using the method of Hodges (1994, 1995, 1999) applied to 850-hPa relative vorticity. To be consistent with models of varying input resolution, and to remove the small-scales of the vorticity field, data are first spectrally truncated to T42, with wavenumbers less than 5 also removed. Tracks are initialized using a nearest neighbor approach and then smoothed via the minimization of a cost function. To ensure only well developed and long-lived, mobile cyclones are analyzed, tracks must exist for at least 48 hr, have a maximum vorticity of least 1×10^{-5} s^{-1}, and travel more than 1000-km from the point of origin.

The cyclone compositing technique used is from Bengtsson et al. (2007); Bengtsson et al. (2009); Catto et al. (2010); Dacre et al. (2012); Sinclai et al. (2020). In order to focus on similar, well developed cyclones.

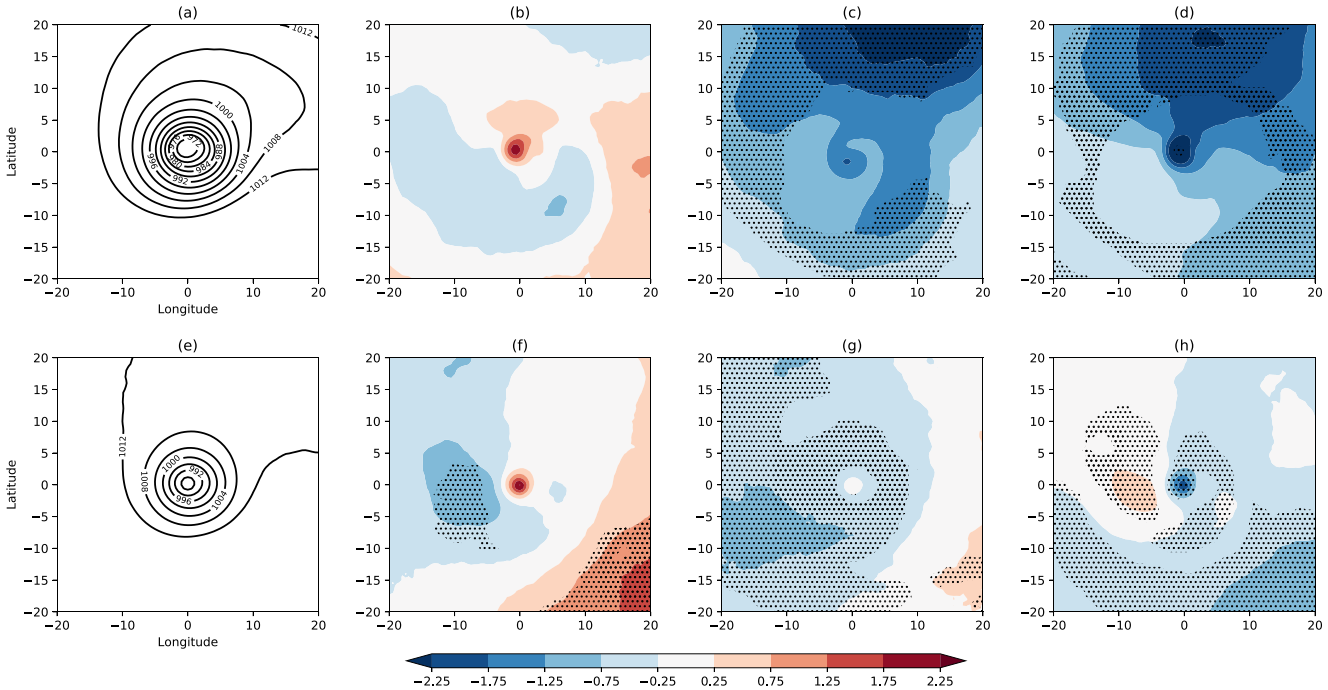

Figure 1. Composites of mean sea level pressure in the northern hemisphere for December, January, February (a–d) and June, July, August (e–h). Composites are shown for ERA5 (a,e) with contours every 4-hPa. Biases relative to ERA5 are shown for the CMIP6 (b,f) and HighResMIP models (c,g). Differences between HighResMIP and CMIP6 are shown in (d,h). Stippling in panels indicates where there is 80% model agreement on the sign of the bias. Units are hPa.

Only cyclones that are in the top 10% of the distribution for peak cyclonic vorticity are analyzed. For ERA5 this equates to an average of 48.1 and 42.8 cyclones per season in the NH for DJF and JJA respectively. Composites are produced for each season year of each model. For each season, hemisphere, and model, a unique vorticity threshold is calculated for the 1979–2014 period to account for seasonality and model variability. To account for variances in cyclone propagation, all fields are rotated and aligned such that all cyclones are traveling from west to east. Composites of MSLP and winds are created at the time of peak vorticity for a 20° region surrounding the cyclone and centered on the track point. Wind speed composites (and the u and v components) at 850-hPa and 250-hPa are examined in a system relative perspective, whereby the propagation speed of the cyclone (calculated as the speed of the rotated cyclone from west to east) is subtracted from the wind speed to identify the winds associated with the cyclone and therefore removing variability introduced from differing propagation speeds in the different model groups (Figure S1 in Supporting Information S1).

3. Results

3.1. Surface Structure

For evaluating the surface structure and shape of ETCs, MSLP is used. In NH DJF the composite cyclone has a 10°-15° radius from the cyclone center (shown by the outer closed contour), which is well captured by the CMIP6 models (Figures 1a and 1b). However, ETCs tend to be too shallow with a minimum pressure of 970.1 hPa, compared to 968.3 hPa in ERA5 ($p < 0.05$). Models tend to vary considerably in their surface structure and cyclone depth (Figure S2 in Supporting Information S1), hence the limited consensus in Figure 1b. HighResMIP models tend to have a lower MSLP minimum than CMIP6 models, with an average simulated minimum of 967 hPa (Figure 1c), which is significantly deeper than ERA5 ($p < 0.05$). Furthermore, MSLP in HighResMIP models is lower across most of the cyclone area, particularly to the north. This is mainly a result of the CMCC-CM2-VHR4 model (Figure S3 in Supporting Information S1) simulating ETCs that are too deep by over 5 hPa and also being situated in a meridional pressure gradient that is considerably stronger than any of the other models.

For both model groups the sign of the MSLP bias is not robust across models at the cyclone center, or the surrounding 10°. Examining the biases individually (Figures S2, S3 in Supporting Information S1) there is considerable variation in the MSLP biases suggesting that cyclone shape and surface structure is very model dependent. Despite this, HighResMIP models do simulate robustly deeper MSLP than CMIP6, indicating the influence of higher resolution. Furthermore, comparing the low and high resolution versions of HighResMIP (not shown) also confirms that the higher resolution models systematically simulate ETCs with deeper MSLP, even when excluding the outlier CMCC models (968.4 hPa low-res and 967 hPa high-res).

In JJA the average cyclone is smaller than in DJF and the closed contour area lies within ∼5° of the cyclone center (Figure 1e). The minimum MSLP in ERA5 is 986.1 hPa, and therefore substantially weaker than in DJF. As in DJF, the CMIP6 models struggle to capture the depth of the ETCs, with the minimum MSLP being significantly too high ($p < 0.05$) with an average of 988.3 hPa (Figure 1f). ETCs in the HighResMIP models (Figures 1g and 1h) simulate an average minimum MSLP of 986.3 hPa, which is not significantly different from ERA5. As in DJF the direct impact of resolution is notable when comparing the HighResMIP models to their lower resolution counterparts, which have significantly lower minimum MSLP ($p < 0.01$), with an average of 987.9 hPa (not shown).

In the SH (Figure S4 in Supporting Information S1) ETC size and structure is more consistent between the two seasons than in the NH. With regards to the minimum MSLP a similar pattern of biases is seen as in the NH. CMIP6 model ETCs are too shallow by 0.75–1.5 hPa, while HighResMIP models simulate a composite cyclone that is up to 0.5 hPa too deep. Furthermore, there is continued evidence that CMIP6 models have a different and variable structure of the MSLP field compared to ERA5, with lower pressures and variable signs of bias away from the cyclone center, which is suggestive of a broader meridional extent of the cyclone and possible wider trough in which the cyclones are situated. This is a feature that is largely reduced in the HighResMIP models, although models are still inconsistent in the sign of bias (Figures S4d, S4h in Supporting Information S1).

3.2. Lower Tropospheric Winds

The CCB (Carlson, 1980; Schultz, 2001) can be identified in cyclone composites of system relative winds at 850-hPa (Figure 2a) traveling rearwards relative to cyclone propagation, polewards of the center. In ERA5 the peak wind speed in this region is above 35 m s^{-1} in NH DJF (Figure 2a) and at least 24.5 m s^{-1} in NH JJA (Figure 2e). CMIP6 models robustly underestimate the strength of this airstream by over 2 m s^{-1} across large areas poleward and rearward of the cyclone within 5° of the cyclone center (Figure 2b), consistent with the weaker pressure gradient (Figure 1). This bias is largest on the westward flank of the cyclone where the CCB tends to fully wrap around the cyclone, forming the low level jet (Schultz, 2001). In the HighResMIP models there is a slight under-estimation to the northeast of the cyclone center, however, there is a large improvement compared to CMIP6 on the western flank (Figure 2c), indicating an improvement in the CCB and low-level jet representation in HighResMIP models (Figure 2d). The lower resolution variants of the HighResMIP models are characterized by the same pattern of biases (not shown) but with a magnitude that is between the HighResMIP and full compliment of CMIP6 models, further demonstrating the direct impact of improved resolution.

In JJA (Figures 2d–2h) a very consistent pattern emerges, with CMIP6 models robustly underestimating the wind strength in the lower troposphere, with minimal biases in the HighResMIP models (Figures 2f–2h). In JJA, due to the weaker nature of the cyclones the cyclonic wrapping of air is less apparent in the difference field (Figures 2f–2h), with biases that are more symmetric around the cyclone center. In the earth relative perspective (Figure S5 in Supporting Information S1) similar differences between model groups are evident, but due to the additional component of the winds due to cyclone propagation, only the bias associated with the wrapping of the CCB on the rear flank of the cyclones is evident.

Biases for DJF and JJA in the SH (Figure S6 in Supporting Information S1) are almost identical to NH DJF, with a magnitude of biases in CMIP6 and HighResMIP that reflects those identified in the NH. Despite improvements in the representation of MSLP minima and lower tropospheric winds in HighResMIP, there are minimal improvements in the structural bias of cyclone track density relative to CMIP6 (Priestley et al., 2020) for NH DJF (Figure S7 in Supporting Information S1) or any other season in either hemisphere, suggesting that these improvements are not due to different geographical locations of the cyclones.

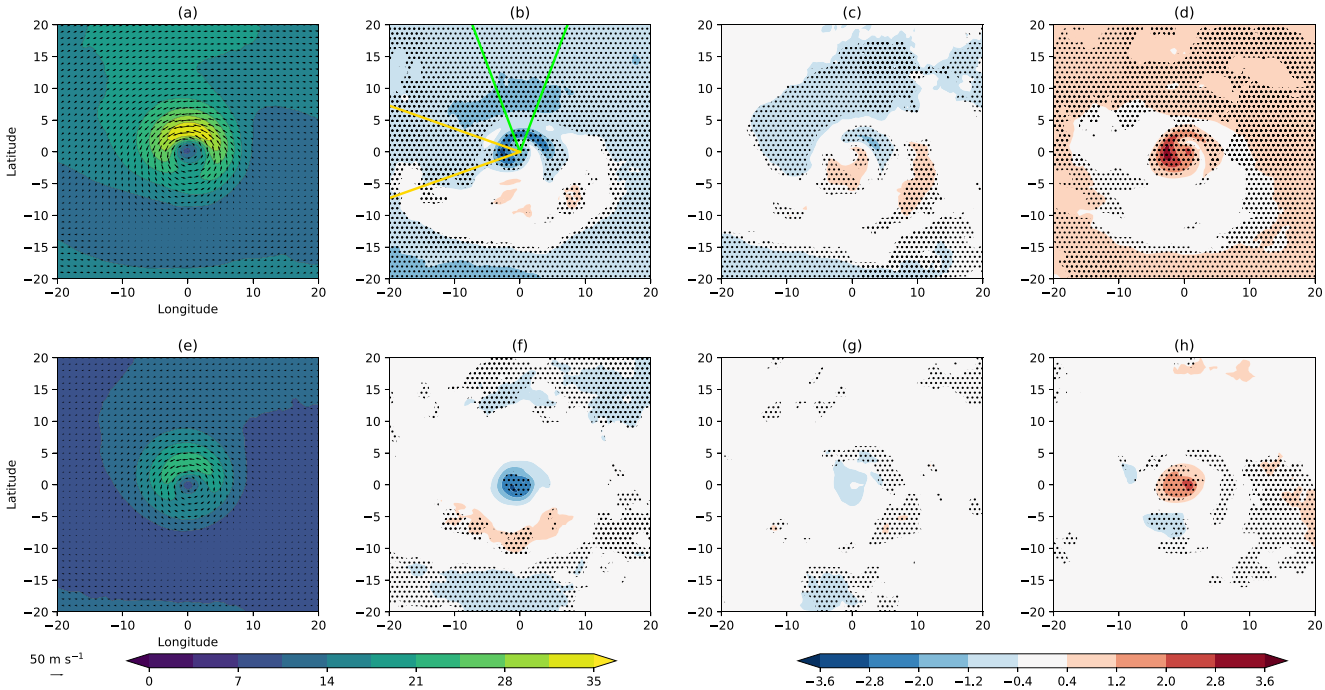

Figure 2. Composites of 850-hPa system relative wind speed in the northern hemisphere for December, January, February (a–d) and June, July, August (e–h). Composites are shown for ERA5 (a,e). Biases relative to ERA5 are shown for the standard CMIP6 models (b,f) and the HighResMIP models (c,g). Differences between HighResMIP and CMIP6 are shown in (d,h). Units are m s^{-1}. The green (70°-110° anticlockwise from due East) and yellow (160°–200°) sectors in (b) are those used for the analysis in Figure 3. Stippling in panels indicates where there is 80% model agreement on the sign of the bias.

3.3. CCB Variability

To quantify variability across the models a Gaussian kernel density estimation of the maximum wind speed and its distance from cyclone center in two sectors at 850-hPa for each seasonal composite cyclone has been performed. The first sector focuses on the winds on the poleward flank of the cyclone, and the second on the bias associated with the wrapping around of the CCB to form the low-level jet on the rear flank (green and yellow sectors in Figure 2b). Focusing on the maxima of the 850-hPa wind speeds, there are two clusters in the ERA5 data (Figure 3a), which are mainly a result of the 0.5° composite resolution. The largest is ∼3° from the center with speeds of ∼35.5 m s^{-1} and the second situated ∼3.5° from the center, with weaker winds. In CMIP6 models most of the cyclones have maxima too far from the cyclone center and too weak by over 1 m s^{-1} (as in Figure 2b). The HighResMIP models capture both the ERA5 clusters, although tend to have a higher proportion of data in the weaker and more distant cluster. There is also a peak even further from the cyclone center with even weaker winds in CMIP6. This suggests that if models simulate a circulation that is too weak, it is also too far from the cyclone center and that only a small number of cyclones (<10%) in CMIP6 simulate the strongest winds sufficiently close to the cyclone center.

In JJA (Figure 3b) a similar pattern is evident, however HighResMIP models tend to have a higher proportion of cyclones with a circulation close to the cyclone center. However, they are still too weak by ∼1 m s^{-1} (as noted in Figure 2c). A majority of cyclones in CMIP6 have too weak and distant circulations, although ∼20% do simulate the correct distance/wind speed. Conversely, a similar proportion are also considerably further from the center and too weak.

On the rear flank of the cyclones in DJF (Figure 3c) there are two groupings in ERA5 at 3° and 3.5° from the cyclone center with speeds of ∼30 m s^{-1}. The HighResMIP models reproduce this distribution very well and capture both groups (as in Figure 2). Some CMIP6 cyclones (∼5%) do capture the intensity distance maxima of ERA5 and HighResMIP, however the majority of CMIP6 cyclones have maximum winds too far from the cyclone center and too weak relative to both HighResMIP and ERA5. Furthermore, there is a grouping of ∼30% of CMIP6 cyclones that are substantially further from the cyclone center (∼ 4.75°) and too weak by 3–5 m s^{-1}.

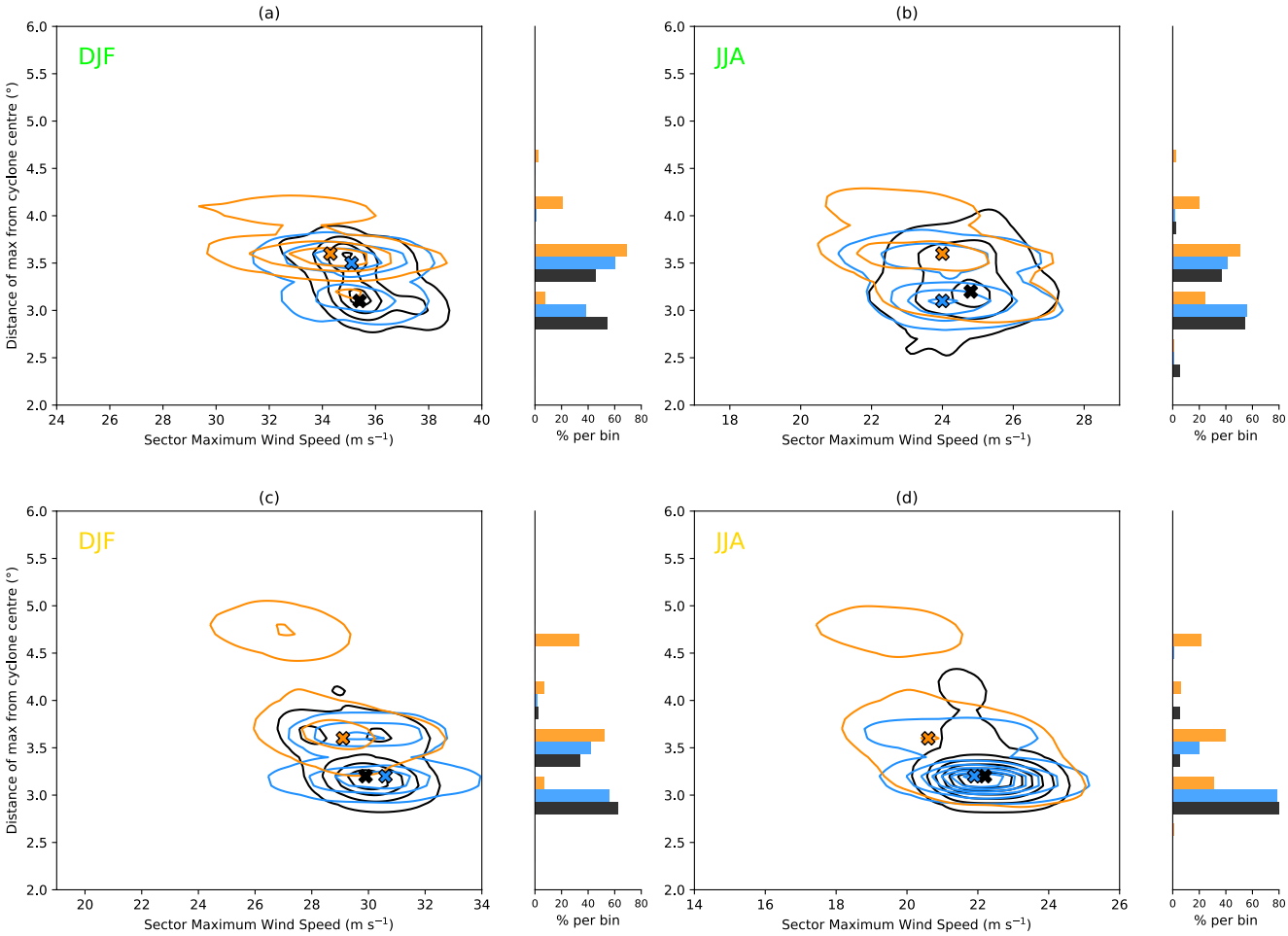

Figure 3. Gaussian kernel density estimation (KDE) of scattered maximum wind speed against its distance from the cyclone center for sectors from (a–b) 70°-110° and (c–d) 160°-200° in (a,c) December, January, February and (b,d) June, July, August for the northern hemisphere. KDEs are shown for ERA5 (black), CMIP6 (orange) and HighResMIP (blue). Crosses indicate the maximum density of each KDE. Degrees for the sectors are moving anticlockwise around the cyclone, with 0° representing East and are illustrated in Figure 2b. Contours levels are from 0.05 to 0.95 in intervals of 0.15.

This indicates that for CMIP6 models that fail to capture the strength of the wind speeds, the associated airstream will be situated further from the cyclone center ($r = -0.57$). These patterns and groupings continue to be evident in JJA (Figure 3d), with performances of HighResMIP and CMIP6 models being similar to DJF.

3.4. Upper Tropospheric Winds

In the upper-troposphere (250-hPa) ETCs are commonly characterized by reduced ascent on their equatorward and forward flanks relative to lower levels (Figure S8 in Supporting Information S1), with a more horizontal flow that is associated with the outflow of the WCB near the tropopause (Dacre et al., 2012; Sinclair et al., 2020). Two branches of the WCB are commonly identifiable that turn cyclonically and anticyclonically (Browning & Roberts, 1994; Thorncroft et al., 1993) and diverge in the upper troposphere (as in Catto et al., 2010). The dominant feature identified in the system relative winds in ERA5 (Figures 4a and 4e) is the upper-level jet, which has a maximum speed of at least 50 m s^{-1} in DJF and rotates cyclonically around the cyclone from the northwest to the southern flank. A similar picture is present in JJA (Figure 4e), except with a weaker jet that has a maximum of over 30 m s^{-1}. The overall circulation is cyclonic around the center, however, anticyclonic motion is evident to the southeast of the cyclone center that is associated with the WCB outflow.

The CMIP6 models robustly underestimate wind speeds immediately southeast and east of the cyclone center in DJF by up to 3.6 m s^{-1} (Figure 4b). This bias is located close to the region of maximum ascent (Figure S8 in

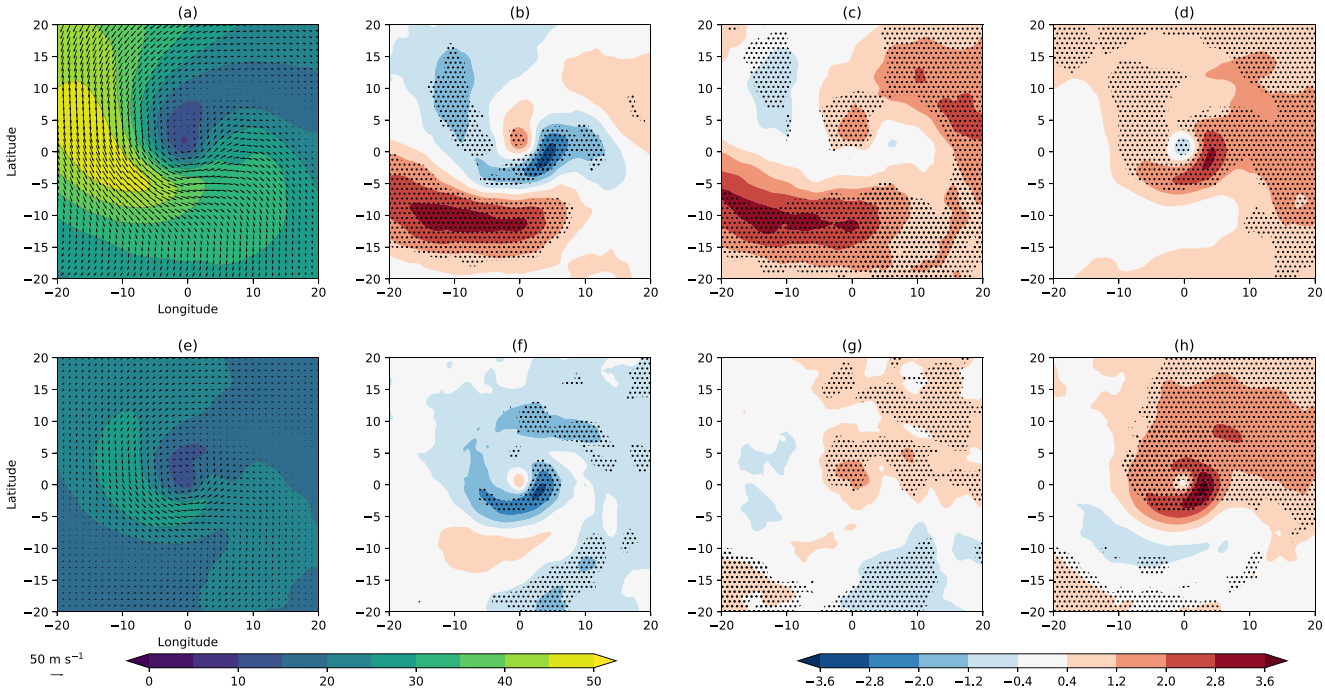

Figure 4. As Figure 2 but for system relative wind speeds at 250-hPa.

Supporting Information S1). This bias, coupled with the models underestimating lower-level convergence and upper-level divergence (Figure S9 in Supporting Information S1) in the region of maximum ascent (Figure S8 in Supporting Information S1) suggests that the ascending WCB is incorrectly represented in the CMIP6 models.

One dominant feature in the CMIP6 composites (Figure 4b) is a positive bias 5°-15° equatorward of the cyclone of up to 3.6 m s^{-1}. This is a result of the jet being too broad and is largely driven by an overly strong zonal component of the wind (Figure S10 in Supporting Information S1), indicating errors in the large-scale jet structure. However, this feature is outside the core cyclone area (as identified in Figure 1a) so the bias is not directly related to the cyclones.

The HighResMIP models feature considerably reduced biases to the south and east of the cyclone center (Figures 4c and 4d). Therefore, higher resolution is likely contributing to an improved representation of the ascending branch of the cyclones and the increased upper-level divergence relative to CMIP6 (Figure S9h in Supporting Information S1) implies stronger vertical velocities. The HighResMIP models also over-estimate winds 5°-15° equatorward of the ETCs, associated with a too broad zonal component of the jet (Figure S10c in Supporting Information S1), suggesting that this bias is not improved with additional atmospheric resolution. Furthermore, both HighResMIP and CMIP6 models feature an under-estimation of wind speeds to the north-west of the cyclone in the cold sector. This is a region where winds are northerly and is commonly associated with the origins of the descending DI and therefore the region of descent within the cyclone may be incorrectly represented.

One bias that is only evident when isolating the different wind components is the models' failure to represent the anticyclonic turning of winds to the southeast of cyclones. The northerly wind is robustly under-estimated by over 3.6 m s^{-1}, with no improvement notable in the HighResMIP models (Figure S11 in Supporting Information S1). This bias does not appear in the full wind due to the overly strong zonal component of the wind that characterizes the equatorward side of the cyclone. Consequently, the wind speed appears correct in this sector, but the orientation of the wind vectors is incorrect and the large-scale flow is overly zonal (consistent with Priestley et al., 2020).

In JJA the models have similar characteristics to DJF (Figures 4f–4h). The broader zonal component of the wind is still present, but considerably weaker in JJA (Figures 4f and 4g), and therefore the band of increased wind

speeds to the south of the cyclone is less clear. CMIP6 models continue to robustly underestimate the strength of the winds to the southeast and east of the cyclone center, with HighResMIP improved relative to CMIP6 (Figures 4g and 4h). The anticyclonic circulation to the southeast of cyclones is less evident in JJA as cyclones are weaker. However, both CMIP6 and HighResMIP continue to have biases associated with the anticyclonic part of the circulation (Figure S11 in Supporting Information S1).

All biases present in the NH are identifiable with similar magnitudes and locations in the SH (Figure S12 in Supporting Information S1). The zonal component of the jet continues to be too broad and the winds associated with the WCB outflow are too weak in CMIP6 models, with improvements notable in HighResMIP models. Furthermore, all models insufficiently represent the anticyclonic flow to the northeast of cyclones.

4. Discussion and Conclusions

In this study the benefits of high resolution modeling on simulating ETC structure and circulation are explored and quantified using the HighResMIP and CMIP6 models. The main conclusions are as follows:

1. CMIP6 models generally capture the features of ETCs, however the shape and structure of the surface cyclone is very model dependent, and cyclone wind speeds throughout the troposphere tend to be too weak.
2. HighResMIP models decrease most of the biases in CMIP6 models at the cyclone scale. Wind speeds in the lower and upper troposphere are stronger and surface pressures deeper.
3. Large-scale features of the cyclone environment are not improved with increased resolution. These are an overly broad and zonal jet, and an insufficient anticyclonic turning of the flow to the southeast of cyclones in the upper-troposphere.

Despite improvements in the representation of a majority of the cyclone features in the winter and summer seasons of the NH and SH, there are minimal improvements in the geographical distribution of cyclones in HighResMIP models relative to CMIP6 (Figure S7 in Supporting Information S1). Generally, all biases associated with the CCB and the inflow and ascent of the WCB in CMIP6 are reduced, and are associated with a deeper surface cyclone, in HighResMIP. Previous studies such as Bengtsson et al. (2009) and Booth et al. (2018) found improved representation of cyclones with higher resolution, and the HighResMIP models have been noted to have considerable benefits compared to standard resolution CMIP6 models in terms of explosive ETC wind speed and tropical cyclone intensity (Jiaxiang et al., 2020; Roberts et al., 2020), which we add further evidence to in this study, with the models offering improvements over their lower resolution counterparts. Improved resolution has also shown to be important in future projections, with higher resolution models projecting greater storminess in the North Atlantic by the end of the century (Grist et al., 2021). Therefore, a key research directive should be to assess what processes associated with higher resolution are driving the improvements in HighResMIP models.

Associated with the negative wind speed biases and underestimation of divergence in the WCB outflow region in CMIP6 models (and subsequent improvement in HighResMIP) it is likely that ascent rates are too weak in CMIP6 models (as in Naud et al., 2010; Govekar et al., 2014), or that the outflow is at the wrong level or ascent in the wrong place. Too weak ascent is a common problem in models which often have insufficient representation of diabatic processes and strong temperature gradients (Willison et al., 2013), which contribute to the ascent in the WCB (Kuo et al., 1991). As HighResMIP models likely offer an improved representation of diabatic processes it is likely that there are also improvements in the ascent rate of the WCBs relative to CMIP6.

CMIP6 models have variable performance for the strength of simulated wind speeds. When wind speeds are too weak the associated airstreams tend to be further from the cyclone center, and likely broader than in ERA5 and HighResMIP. Overall, the structure and circulation biases in CMIP6 are somewhat similar to other modeling studies, with CMIP6 models simulating the correct features at the correct vertical levels within the cyclone (Catto et al., 2010; Kodama et al., 2019; Sinclair et al., 2020). Models particularly struggle in reproducing the structure of the surface cyclone and the associated MSLP depth, with a variety of structures evident across both the CMIP6 and HighResMIP models. As MSLP is strongly influenced by large-scale patterns (Hoskins & Hodges, 2002) it is unlikely to provide consistent results with regards to cyclone size, surface structure/shape, or peak intensity.

HighResMIP models show improvements over CMIP6 and their lower resolution counterparts on the cyclone scale, yet do not reduce biases on the large-scale, such as the overly broad and zonal jet, the reduced anticyclonic

turning of air associated with the WCB near the tropopause, and the equatorward flow of air behind the cold front that may associated with the DI and insufficient descent. Errors associated with the WCB turning may be linked to the representation of the stratosphere and its interaction with the troposphere. None of the HighResMIP models have an increase in vertical resolution compared to their standard resolution models, and therefore are not likely to feature improvements in stratosphere-troposphere interactions. Increases in vertical resolution may be required to aid the improvements noted with horizontal resolution.

Data Availability Statement

ERA5 reanalysis is available from the Copernicus Climate Change Service Climate Data Store (https://doi.org/10.24381/cds.bd0915c6). CMIP6 and HighResMIP data is publicly available through the Earth System Grid Federation (https://esgf-node.llnl.gov/projects/cmip6/). The CMIP6 and HighResMIP models used in this study are listed in Tables S1 and S2 respectively of the Supporting Information. The cyclone tracking and compositing algorithm TRACK is available on request from Kevin Hodges at https://gitlab.act.reading.ac.uk/track/track.

Acknowledgments
M. D. K. Priestley and J. L. Catto are supported by the Natural Environment Research Council (NERC) grant NE/S004645/1. We would like to thank the two anonymous reviewers, whose helpful and constructive feedback helped improve this manuscript.

References

Bengtsson, L., Hodges, K. I., Esch, M., Keenlyside, N., Kornblueh, L., Luo, J.-J., & Yamagata, T. (2007). How may tropical cyclones change in a warmer climate? *Tellus A: Dynamic Meteorology and Oceanography*, *59*(4), 539–561. https://doi.org/10.1111/j.1600-0870.2007.00251.x

Bengtsson, L., Hodges, K. I., & Keenlyside, N. (2009). Will extratropical storms intensify in a warmer climate? *Journal of Climate*, *22*(9), 2276–2301. https://doi.org/10.1175/2008JCLI2678.1

Booth, J. F., Naud, C. M., & Willison, J. (2018). Evaluation of extratropical cyclone precipitation in the North Atlantic basin: An analysis of ERA-interim, WRF, and two CMIP5 models. *Journal of Climate*, *31*(6), 2345–2360. https://doi.org/10.1175/JCLI-D-17-0308.1

Browning, K. A. (1997). The dry intrusion perspective of extra-tropical cyclone development. *Meteorological Applications*, *4*(4), 317–324. https://doi.org/10.1017/S1350482797000613

Browning, K. A. (2004). The sting at the end of the tail: Damaging winds associated with extratropical cyclones. *Quarterly Journal of the Royal Meteorological Society*, *130*(597), 375–399. https://doi.org/10.1256/qj.02.143

Browning, K. A., & Roberts, N. M. (1994). Structure of a frontal cyclone. *Quarterly Journal of the Royal Meteorological Society*, *120*(520), 1535–1557. https://doi.org/10.1002/qj.49712052006

Carlson, T. N. (1980). Airflow through midlatitude cyclones and the comma cloud pattern. *Monthly Weather Review*. *108*, 1498–1509. https://doi.org/10.1175/1520-0493(1980)108<1498:atmcat>2.0.co;2

Catto, J. L. (2016). Extratropical cyclone classification and its use in climate studies. *Reviews of Geophysics*, *54*(2), 486–520. https://doi.org/10.1002/2016RG000519

Catto, J. L., & Dowdy, A. (2021). Understanding compound hazards from a weather system perspective. *Weather and Climate Extremes*, *32*, 100313. https://doi.org/10.1016/j.wace.2021.100313

Catto, J. L., Shaffrey, L. C., & Hodges, K. I. (2010). Can climate models capture the structure of extratropical cyclones? *Journal of Climate*, *23*(7), 1621–1635. https://doi.org/10.1175/2009JCLI3318.1

Colle, B. A., Zhang, Z., Lombardo, K. A., Chang, E., Liu, P., & Zhang, M. (2013). Historical evaluation and future prediction of eastern North American and western Atlantic extratropical cyclones in the CMIP5 models during the cool season. *Journal of Climate*, *26*(18), 6882–6903. https://doi.org/10.1175/JCLI-D-12-00498.1

Dacre, H. F., Hawcroft, M. K., Stringer, M. A., & Hodges, K. I. (2012). An extratropical cyclone Atlas: A tool for illustrating cyclone structure and evolution characteristics. *Bulletin of the American Meteorological Society*, *93*(10), 1497–1502. https://doi.org/10.1175/BAMS-D-11-00164.1

Eyring, V., Bony, S., Meehl, G. A., Senior, C. A., Stevens, B., Stouffer, R. J., & Taylor, K. E. (2016). Overview of the coupled model Intercomparison project phase 6 (CMIP6) experimental design and organization. *Geoscientific Model Development*, *9*(5), 1937–1958. https://doi.org/10.5194/gmd-9-1937-2016

Field, P. R., & Wood, R. (2007). Precipitation and cloud structure in midlatitude cyclones. *Journal of Climate*, *20*(2), 233–254. https://doi.org/10.1175/JCLI3998.1

Govekar, P. D., Jakob, C., & Catto, J. (2014). The relationship between clouds and dynamics in Southern Hemisphere extratropical cyclones in the real world and a climate model. *Journal of Geophysical Research: Atmospheres*, *119*(11), 6609–6628. https://doi.org/10.1002/2013JD020699

Grist, J. P., Josey, S. A., Sinha, B., Catto, J. L., Roberts, M. J., & Coward, A. C. (2021). Future evolution of an eddy rich ocean associated with enhanced east Atlantic storminess in a coupled model projection. *Geophysical Research Letters*, *48*(7), e2021GL092719. https://doi.org/10.1029/2021GL092719

Haarsma, R. J., Roberts, M. J., Vidale, P. L., Senior, C. A., Bellucci, A., Bao, Q., et al. (2016). High resolution model Intercomparison project (HighResMIP v1.0) for CMIP6. *Geoscientific Model Development*, *9*(11), 4185–4208. https://doi.org/10.5194/gmd-9-4185-2016

Harrold, T. W. (1973). Mechanisms influencing the distribution of precipitation within baroclinic disturbances. *Quarterly Journal of the Royal Meteorological Society*, *99*(420), 232–251. https://doi.org/10.1002/qj.49709942003

Hawcroft, M. K., Shaffrey, L. C., Hodges, K. I., & Dacre, H. F. (2016). Can climate models represent the precipitation associated with extratropical cyclones? *Climate Dynamics*, *47*(3), 679–695. https://doi.org/10.1007/s00382-015-2863-z

Hersbach, H., Bell, B., Berrisford, P., Hirahara, S., Horányi, A., Muñoz-Sabater, J., et al. (2020). The ERA5 global reanalysis. *Quarterly Journal of the Royal Meteorological Society*, *146*(730), 1999–2049. https://doi.org/10.1002/qj.3803

Hodges, K. I. (1994). A general method for tracking analysis and its application to meteorological data. *Monthly Weather Review*. *122*, 2573–2586. https://doi.org/10.1175/1520-0493(1994)122<2573:agmfta>2.0.co;2

Hodges, K. I. (1995). Feature tracking on the unit sphere. *Monthly Weather Review*. *123*, 3458–3465. https://doi.org/10.1175/1520-0493(1995)123<3458:ftotus>2.0.co;2

Hodges, K. I. (1999). Adaptive constraints for feature tracking. *Monthly Weather Review*. *127*, 1362–1373. https://doi.org/10.1175/1520-0493(1999)127<1362:acfft>2.0.co;2

Hoskins, B. J., & Hodges, K. I. (2002). New perspectives on the Northern hemisphere winter storm tracks. *Journal of the Atmospheric Sciences*. *59*, 1041–1061. https://doi.org/10.1175/1520-0469(2002)059<1041:npotnh>2.0.co;2

Jiaxiang, G., Shoshiro, M., Roberts, M. J., Haarsma, R., Putrasahan, D., Roberts, C. D., et al. (2020). Influence of model resolution on bomb cyclones revealed by HighResMIP-PRIMAVERA simulations. *Environmental Research Letters*, *15*(8), 084001. https://doi.org/10.1088/1748-9326/ab88fa

Jung, T., Miller, M. J., Palmer, T. N., Towers, P., Wedi, N., Achuthavarier, D., et al. (2012). High-resolution global climate simulations with the ECMWF model in project athena: Experimental design, model climate, and seasonal forecast skill. *Journal of Climate*, *25*(9), 3155–3172. https://doi.org/10.1175/JCLI-D-11-00265.1

Kodama, C., Stevens, B., Mauritsen, T., Seiki, T., & Satoh, M. (2019). A new perspective for future precipitation change from intense extratropical cyclones. *Geophysical Research Letters*, *46*(21), 12435–12444. https://doi.org/10.1029/2019GL084001

Kuo, Y., Shapiro, M. A., & Donall, E. G. (1991). The interaction between baroclinic and diabatic processes in a numerical simulation of a rapidly intensifying extratropical marine cyclone. *Monthly Weather Review*. (Vol. *119*, pp. 368–384). https://doi.org/10.1175/1520-0493(1991)119<0368:tibbad>2.0.co;2

Naud, C. M., Genio, A. D. D., Bauer, M., & Kovari, W. (2010). Cloud vertical distribution across warm and cold fronts in CloudSat-CALIPSO data and a general circulation model. *Journal of Climate*, *23*(12), 3397–3415. https://doi.org/10.1175/2010JCLI3282.1

Pfahl, S., & Wernli, H. (2012). Quantifying the relevance of cyclones for precipitation extremes. *Journal of Climate*, *25*(19), 6770–6780. https://doi.org/10.1175/JCLI-D-11-00705.1

Priestley, M. D. K., Ackerley, D., Catto, J. L., Hodges, K. I., McDonald, R. E., & Lee, R. W. (2020). An overview of the extratropical storm tracks in CMIP6 historical simulations. *Journal of Climate*, *33*(15), 6315–6343. https://doi.org/10.1175/JCLI-D-19-0928.1

Raveh-Rubin, S. (2017). Dry intrusions: Lagrangian climatology and dynamical impact on the planetary boundary layer. *Journal of Climate*, *30*(17), 6661–6682. https://doi.org/10.1175/JCLI-D-16-0782.1

Roberts, M. J., Camp, J., Seddon, J., Vidale, P. L., Hodges, K., Vanniere, B., et al. (2020). Impact of model resolution on tropical cyclone simulation using the HighResMIP-PRIMAVERA multimodel ensemble. *Journal of Climate*, *33*(7), 2557–2583. https://doi.org/10.1175/JCLI-D-19-0639.1

Schiemann, R., Athanasiadis, P., Barriopedro, D., Doblas-Reyes, F., Lohmann, K., Roberts, M. J., et al. (2020). Northern hemisphere blocking simulation in current climate models: Evaluating progress from the climate model Intercomparison project phase 5 to 6 and sensitivity to resolution. *Weather and Climate Dynamics*, *1*(1), 277–292. https://doi.org/10.5194/wcd-1-277-2020

Schultz, D. M. (2001). Reexamining the cold conveyor belt. *Monthly Weather Review*. *129*, 2205–2225. https://doi.org/10.1175/1520-0493(2001)129<2205:rtccb>2.0.co;2

Schultz, D. M., Bosart, L. F., Colle, B. A., Davies, H. C., Dearden, C., Keyser, D., et al. (2019). Extratropical cyclones: A century of research on meteorology's centerpiece. *Meteorological Monographs*, *59*, 16–116. https://doi.org/10.1175/AMSMONOGRAPHS-D-18-0015.1.56

Sinclair, V. A., Rantanen, M., Haapanala, P., Räisänen, J., & Järvinen, H. (2020). The characteristics and structure of extra-tropical cyclones in a warmer climate. *Weather and Climate Dynamics*, *1*(1), 1–25. https://doi.org/10.5194/wcd-1-1-2020

Taylor, K. E., Juckes, M., Balaji, V., Cinquini, L., Denvil, S., Durack, P. J., et al. (2017). *CMIP6 global attributes, DRS, filenames, directory structure and, CV's (Tech. Rep. No. v6.2.6)*. Retrieved from https://goo.gl/v1drZl: Program for Climate Model Diagnosis and Intercomparison

Thorncroft, C. D., Hoskins, B. J., & McIntyre, M. E. (1993). Two paradigms of baroclinic-wave life-cycle behaviour. *Quarterly Journal of the Royal Meteorological Society*, *119*(509), 17–55. https://doi.org/10.1002/qj.49711950903

Willison, J., Robinson, W. A., & Lackmann, G. M. (2013). The importance of resolving mesoscale latent heating in the North Atlantic storm track. *Journal of the Atmospheric Sciences*, *70*(7), 2234–2250. https://doi.org/10.1175/JAS-D-12-0226.1